Methods for monitoring and controlling multi-rotor micro-UAVs position and orientation based on LabVIEW

Siyu Pei[1], Shizhou Wang[2], Huihui Zhang[3], Hang Zhu[1*]

(1. *School of Mechanical and Aerospace Engineering, Jilin University, Changchun 130022, China*;
2. *National Center for International Collaboration Research on Precision Agricultural Aviation Pesticides Spraying Technology, Guangzhou 5146042, China*;
3. *USDA-ARS, Water Management and Systems Research Unit, Collins, CO 80526, USA*)

Abstract: The multi-rotor micro-UAV has become an important platform for assessing crop information promptly given its high flexibility, compact size, low cost, and high spatial resolution. However, considering the limits of the stability of the micro-UAV control system and the precision of automatic navigation systems, how to timely adjust the position and attitude of UAVs to ensure the target within the scope of monitoring is one of the key techniques which determines whether micro-UAVs can be widely used in precision agriculture as a remote sensing platform. In this study, the integrated navigation system of INS/GPS (Inertial Navigation System/Global Positioning System) and EKF (Extended Kalman Filter) was adopted as the navigation system and fusion algorithm for simulation analysis respectively, to monitor the position and attitude of UAVs more accurately and thus improve the estimation accuracy and control precision. An autonomous flight experiment was designed and carried out, and experimental data collected by commercially available UAVs. LabVIEW was used to analyze and process all experimental data and outputted flight state graphs, which reflected the optimization effect of EKF algorithm and control precision visually.

Keywords: Multi-rotor UAV, navigation system, position and attitude estimation, data fusion, LabVIEW
DOI: 10.33440/j.ijpaa.20180101.0009

Citation: Pei S Y, Wang S Z, Zhang H H, Zhu H. Methods for monitoring and controlling multi-rotor micro-UAVs position and orientation based on LabVIEW. Int J Precis Agric Aviat, 2018; 1(1): 51–58.

1 Introduction

In recent years, with the rapid development of microelectronic control sensor (accelerator, gyroscope, magnetometer, pressure sensor), micro GPS module, microprocessor, and multi-frequency radio, the multi-rotor micro-UAV has been increasingly applied in agriculture[1,2]. It possesses numerous advantages including low cost, small volume, light weight, compact structure, simple operation, high flexibility, and low cost of maintenance and operation. Micro-UAVs have become one of the main methods to obtain crop information with a remote sensing platform, and are an important advancement in order to develop precision agriculture[3,4]. When hovering over the crop based on automatic navigation, location and posture of micro-UAVs will be influenced by the working environment. How to tune the position and attitude of UAVs timely in order to ensure the target within the scope of monitoring is one of the key techniques that determines whether micro-UAVs can become more widely used in precision agriculture as a remote sensing platform. Monitoring the position and attitude of micro-UAVs more accurately will improve the estimation accuracy and thus the control precision.

In order to monitor the position and attitude of micro-UAVs, large amounts of data and images must be provided by the navigation system. In recent years, various navigation systems have been researched, including inertial navigation system (INS), satellite positioning system, and vision navigation system. Among all the navigation systems, the integrated system of INS/GPS has been most widely applied in the field of crop information acquisition given its higher accuracy, faster update frequency, and smaller error accumulation. Sugiura, Noguchi, Ishii, and Terao developed an unmanned helicopter equipped with INS/GPS navigation system and crop status detection system[5]. GPS was used to acquire real-time position information, inertial sensors to provide roll and pitch, and imaging sensors to detect crop status. As the result, a map including 41 cm error could be generated using the image taken by the helicopter[6]. Haitao Xiang and Lei Tian developed an unmanned aerial vehicle to monitor the application of turf grass glyphosate, which used the INS/GPS navigation to provide estimation of position and attitude[7]. They developed a navigation system using inertial measurement unit sensor, global positioning system, and sensor fusion technology to detect the position and attitude of UAV.

For position and attitude detection there is a major technical problem that UAV application and promotion will face in the field of agriculture in China. This problem is how to improve the calculation accuracy of position and attitude with low-cost sensors. Meanwhile, attitude calculation is more complex, and it is more difficult to control attitude. Thus a series of data fusion algorithms was proposed by researchers. The three-axis attitude determination (TRIAD) is a classical algorithm in the early stage, the basic idea of which is using two non-parallel vectors to

Received date: 2018-03-19 **Accepted date:** 2018-06-28
Biographies: Siyu Pei, Undergraduate, research interests: precision agricultural aviation and equipment, Email: Peisiyuxp@163.com; **Shizhou Wang**, PhD, Professor, research interests: precision agricultural aviation application, Email: shwang@scau.edu.cn; **Huihui Zhang,** PhD, Agricultural Engineer, research interests: agricultural aviation application, Email: huihui.Zhang@ars.usda.gov.
*__Corresponding author: Hang Zhu__, PhD, Associate Professor, research interests: intelligent machinery of precision agriculture and automatic control, precision agricultural aviation and equipment. School of Mechanical and Aerospace Engineering, Jilin University NO.5988, Renmin Road, Changchun. China. Email: hangzhu@jlu.edu.cn.

determine the three-axis attitude of the carrier. Black, Lerner, and Shuster estimated the position and attitude of UAVs with TRIAD algorithms in its early developmental stage[8]. Direction cosine matrix (DCM) has been applied in various UAVs for many years as a classical algorithm[9]. Premerlani and Bizard increased the error compensation link of inertial element based on the DCM[10], when they compared the value measured by accelerometer and magnetometer with the recursive results from calibration vector based on DCM algorithm, and obtained the difference value. The value was input as the proportional integral (PI) system[11], and the output was fed back to the attitude calculation in next round as the compensation of gyro error. But during the calculating process it is easily interfered with by noises and influences the final results due to lack of the interference detection link. Lefferts, Markley, and Shuster developed the attitude calculation based on the kalman filtering algorithm and obtained the optimal estimation of system[12]. It can filter the noise from observation data, while the kalman filtering algorithm can achieve position information fusion and calculate the position of the UAV. Psiaki, Martel, and Pal introduced the TRIAD[13] method into an observation equation based on the kalman filtering algorithm, but it would produce numerous matrix operations. Thus Bar-Itzhack and Oshman directly used the measurement vector obtained from accelerometer and magnetometer as the observation value of kalman filter[14]. Kumar, Hall, and Cordova achieved the position and attitude calculation of nonlinear system using the EKF algorithm[15].

In order to obtain an accurate detection of a UAV's position and attitude in the field of agriculture remote sensing information acquisition, we developed the UAV detection system of position and attitude based on INS/GPS integrated navigation system and EKF fusion algorithm of data.

2 Detection system of position and attitude

The position and attitude detection system is applied in the field of agriculture remote sensing, use the UAV as flight platform, record the flight status through the navigation sensors, processing the data using navigation calculation method and data fusion algorithm to get the UAVs flight information of position and attitude. A series of experiments and simulation studies are developed, and the technical route is as shown in Figure 1.

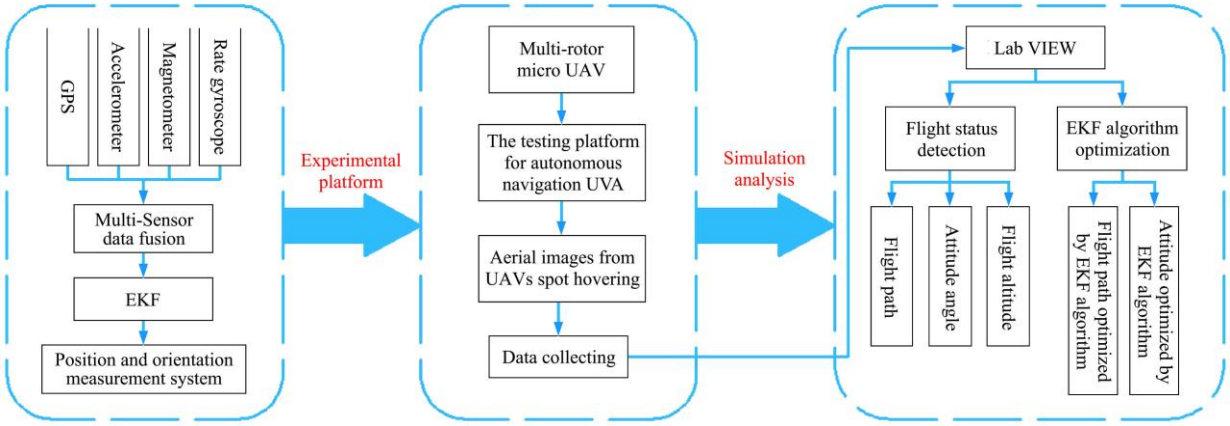

Figure 1 Technical route

2.1 Flight platform of UAVs

At present, the UAVs flight platform applied in the field of agriculture mainly includes fixed-wing UAV and rotor UAV. Fixed-wing UAV is easy to control, possesses good stability, high load bearing ability, but low mobility. And the runway is needed when it lands or takes off. The rotor UAV possesses the excellent mobility, good flexibility and it can achieve vertical takeoff or landing. Thinking of the agriculture condition and costs, we developed a flight platform with DJI Phantom4 advanced, which is a micro multi-motor UAV. The main technical parameters are as shown in Table 1.

Table 1 Main technical parameters of DJI Phantom4 advanced

Parameter	Value
Max Ascent Speed	6 m/s (Sport mode)
Max Descent Speed	4 m/s (Sport mode)
Max Speed	20 m/s (Sport mode))
Max Flight altitude	150 m
Operating Temperature	0-40°C
GPS Mode	GPS/GLONASS
Image Sensor	1/2.3”(CMOS),Effective pixels:12.4M
Lens	FOV 94° 20 mm (35 mm format equivalent) f/2.8 focus at
Photo	JPEG, DNG (RAW)
Image Max Size	4000×3000

2.2 Navigation sensor

In this paper, UAVs position and attitude information was obtained by INS/GPS integrated navigation. The INS need no external signal source, processes independence and high frequency output of UAVs status information, but there will be time dependent errors which increase without bounds. GPS provides accurate position information in a long time, but relatively low output rate of data, and it is easy to be effected by weather, environment and the unstable connection between antenna and satellites. The INS/GPS integrated navigation can overcome the drawbacks for each system. Internal sensors mainly included accelerometers, magnetometer and gyroscope. Accelerometers measured the linear acceleration. The time integration of acceleration obtains velocity, and the second time integration obtains position. Three axis magnetometer measured geomagnetic field component, and the UAVs heading was obtained based on the measured data through calculation formula and the transformations between frames. Rate gyroscope measured the angular velocity, which transformed from Euler angle format to quaternion format and propagated through a difference function to obtain the attitude information of UAV. However, the status information obtained from INS is easy to appear time dependent errors, the correction of these information was by observed value from GPS.

Inertial navigation sensors measured in the body frame, GPS measured in the WGS-84 frame and the navigation frame was

chosen to complete the data fusion, before the calculation of position and attitude and data fusion, transformations between reference frames is necessary. Definitions for those reference frames are shown in Table 2. The transformation between the body frame and the navigation frame was achieved by Eq. (1) (Farrell & Barth, 1998), and the relationship of these frames is shown in Figure 2. The transformation between the WGS-84 frame and the navigation frame need two steps, the first step was transformation from the WGS-84 frame to the Earth-centered Earth-fixed (ECEF) frame using Eqs. (2)-(7) (Farrell & Barth, 1998), the next step was achieved the transformation from the ECEF frame to the navigation frame by Eq. (8) (Farrell & Barth, 1998), and the relationship of these frames is shown in Figure 3.

$$X^e=(\underline{N}+h)\cos\varphi\cos\lambda \tag{1}$$

$$Y^e=(\underline{N}+h)\cos\varphi\sin\lambda \tag{2}$$

$$Z^e=[N(1-e^2)+h]\sin\varphi \tag{3}$$

$$N=a/\sqrt{(1-e^2\sin^2\varphi)} \tag{4}$$

$$f=(a-b)/a \tag{5}$$

$$e^2=2f-f^2 \tag{6}$$

$$T_{ecef}^{ned}=\begin{bmatrix}-\sin\lambda\cos\varphi & -\sin\lambda\sin\varphi & \cos\lambda\\ -\sin\varphi & \cos\varphi & 0\\ -\cos\lambda\cos\varphi & -\cos\lambda\sin\varphi & \sin\lambda\end{bmatrix} \tag{7}$$

where, (ϕ,θ,ψ) is the roll, pitch and yaw obtained through the calculation of angular rates, which measured by gyroscope in the body frame. (X^e, Y^e, Z^e) is the position in the ECEF frame (λ, φ, h) are the latitude, longitude and altitude measured by GPS in the WGS-84 frame; a is the semi-major earth axis with a value of 6378137 m; b is the semi-minor earth axis with a value of 6356752 m. Definitions of reference frames is shown as Rable 2.

Table 2 Definitions of reference frames

Reference Frame	Definition
ECEF Frame	Origin in the earth's center of mass; x-axis points to the intersection of earth equatorial plane and Greenwich meridian; z-axis points to the North Pole; y-axis points to longitude 90° E in the equatorial plane.
WGS-84 Frame	WGS 84 is the reference frame used by the Global Positioning System.
Body Frame	Rigidly attached to the UAV, origin in the UAVs center of mass; *x*-axis points forward through the Longitudinal axis of UAV; *y*-axis points right through the horizontal axis of UAV; *z*-axis points downwards based on the right hand rule.
Navigation Frame	Choose the geographic frame as the navigation frame, origin in the earth surface which vehicle is on, one of the axis is coincidence with geographic vertical. This paper chose the NED frame, *x*-axis points to geographic north; *y*-axis points to geographic east; *z*-axis points downwards towards local ellipsoid vertical.

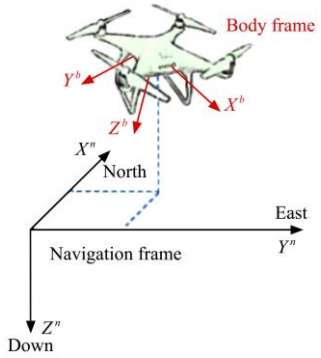

Figure 2 Body and navigation frames

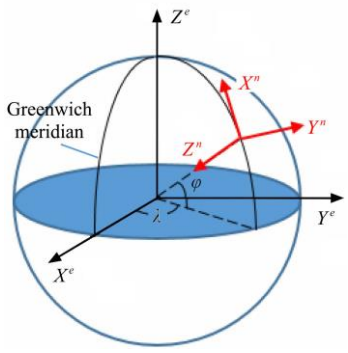

Figure 3 WGS-84, ECEF and navigation frames

$$T_{body}^{ned}=\begin{bmatrix}\cos\theta\cos\psi & -\cos\phi\sin\psi+\sin\phi\sin\theta\cos\psi & \sin\phi\sin\psi+\cos\phi\sin\theta\cos\psi\\ \cos\theta\sin\psi & \cos\phi\cos\psi+\cos\phi\sin\theta\sin\psi & -\sin\phi\cos\psi+\cos\phi\sin\theta\sin\psi\\ -\sin\theta & \sin\phi\cos\theta & \cos\phi\cos\theta\end{bmatrix} \tag{8}$$

2.3 Calculation methods of navigation

UAVs navigation calculation mainly includes attitude, velocity and position calculation. Attitude calculation is using the angular rates from gyroscope solve the Attitude differential equation to obtain the attitude matrix, the attitude information can be abstracted from the matrix. Velocity calculation is obtaining velocity through solving the velocity differential equation based on the acceleration which was measured from accelerometer. The last is position calculation, before calculation, transformation matrix was required to transform the velocity in the body frame into the navigation frame, the matrix was obtained by using the attitude parameters, and the position information was gained based on the continuous integration of the velocity. Among the process of navigation calculation, the attitude was described with the quaternion method. Compared with the methods of Euler angle and direction cosine matrix, the quaternion method has no deadlock problem, less parameters and the calculation is simpler, but it is hardly achieved to describe the attitude change directly. So the attitude output of system was described through the Euler method.

The attitude differential equation described by the quaternion method was shown in Eq. (9) (Farrell & Barth, 1998). The transformation between the quaternion method and Euler method was achieved by Eq. (10)-(12) (Farrell & Barth, 1998). The transformation equation between the body frame and the navigation frame based on the quaternion method was shown in Eq. (13) (Farrell & Barth, 1998).

$$\begin{bmatrix}\dot{q}_0\\ \dot{q}_1\\ \dot{q}_2\\ \dot{q}_3\end{bmatrix}=\frac{1}{2}\begin{bmatrix}-q_1 & -q_2 & -q_3\\ q_0 & -q_3 & q_2\\ q_3 & q_0 & -q_1\\ -q_2 & q_1 & q_0\end{bmatrix}\begin{bmatrix}p\\ q\\ r\end{bmatrix} \tag{9}$$

$$\phi=\arctan\left(\frac{2(q_0q_1+q_2q_3)}{q_0^2-q_1^2-q_2^2+q_3^2}\right) \tag{10}$$

$$\theta=\arcsin(2(q_0q_2-q_1q_3)) \tag{11}$$

$$\psi=\arctan\left(\frac{2(q_0q_3+q_1q_2)}{q_0^2+q_1^2-q_2^2-q_3^2}\right) \tag{12}$$

$$T_{body}^{ned}=\begin{bmatrix} q_0^2+q_1^2-q_2^2-q_3^2 & 2(q_1q_2-q_0q_3) & 2(q_1q_3+q_0q_2) \\ 2(q_1q_2+q_0q_3) & q_0^2-q_1^2+q_2^2-q_3^2 & 2(q_2q_3-q_0q_1) \\ 2(q_1q_3-q_0q_2) & 2(q_2q_3+q_0q_1) & q_0^2-q_1^2-q_2^2+q_3^2 \end{bmatrix} \tag{13}$$

where, (q_0, q_1, q_2, q_3) is the UAVs attitude described by quaternion; ($\dot{q}_0$, $\dot{q}_1$, $\dot{q}_2$, $\dot{q}_3$) is the angular velocity of UAV based on the quaternion method; (p, q, r) are the roll, pitch and yaw angular rates measured by the gyroscope.

The acceleration measured by accelerometer in the body frame is not the true acceleration of UAV, it includes the true UAV acceleration, the acceleration of gravity and the accelerations due to the angular velocity. So the differential equation of UAVs velocity was shown in Eq. (14) (Farrell & Barth, 1998), the differential equation of UAVs position in the navigation frame was shown in Eq. (15).

$$\begin{bmatrix}\dot{u}\\ \dot{v}\\ \dot{w}\end{bmatrix}=\begin{bmatrix}a_x\\ a_y\\ a_z\end{bmatrix}-\begin{bmatrix}0 & -w & v\\ w & 0 & -u\\ -v & u & 0\end{bmatrix}\times\begin{bmatrix}p\\ q\\ r\end{bmatrix}+\begin{bmatrix}2(q_1q_3-q_0q_2)\\ 2(q_2q_3+q_0q_1)\\ q_0^2-q_1^2-q_2^2+q_3^2\end{bmatrix}g \tag{14}$$

$$\begin{bmatrix}\dot{X}\\ \dot{Y}\\ \dot{Z}\end{bmatrix}=\begin{bmatrix}v_n\\ V_e\\ v_d\end{bmatrix}=T_{body}^{ned}\cdot\begin{bmatrix}u\\ v\\ w\end{bmatrix} \tag{15}$$

where, ($\dot{u}$, $\dot{v}$, $\dot{w}$) is the true UAV acceleration along the three axis in the body reference frame; (a_x, a_y, a_z) is the UAV acceleration measured by accelerometer; (u, v, w) is the velocity of UAV; g is the local gravity; (v_n, v_e, v_d) are the velocities along the north, east and downward direction in the navigation frame; (X, Y, Z) is the UVAs position in the navigation frame.

2.4 Mathematical model of stochastic nonlinear continuous system for UAV

The state parameters of system consisted of the position in the navigation frame, the velocity and attitude in the body frame, the bias of the accelerometer and the drifts of the rate gyroscope. The non-linear state equation as following Eq. (16) (Brown & Huang, 1997; Gelb, 1974) was constructed by these parameters. The variables of GPS, accelerometer and magnetometer were directly or indirectly selected to construct the observation equation as following Eq. (17) (Brown & Huang, 1997).

$$\begin{aligned}\dot{X}_s(t)&=[\dot{X}\dot{Y}\dot{Z}\dot{u}\dot{v}\dot{w}\dot{q}_0\dot{q}_1\dot{q}_2\dot{q}_3\dot{b}_p\dot{b}_q\dot{b}_r\dot{b}_{a_x}\dot{b}_{a_y}\dot{b}_{a_z}]^T\\ &=f(x_s,u_m)+\omega\\ &=\begin{bmatrix} T_{body}^{ned}\cdot\begin{bmatrix}u\\ v\\ w\end{bmatrix} \\ \begin{bmatrix}a_x-b_{a_x}\\ a_y-b_{a_y}\\ a_z-b_{a_z}\end{bmatrix}-\begin{bmatrix}u\\ v\\ w\end{bmatrix}\times\begin{bmatrix}p-b_p\\ q-b_q\\ r-b_r\end{bmatrix}+\begin{bmatrix}2(q_1q_3-q_0q_2)\\ 2(q_2q_3+q_0q_1)\\ q_0^2-q_1^2-q_2^2+q_3^2\end{bmatrix}+\omega \\ \frac{1}{2}\begin{bmatrix}-q_1 & -q_2 & -q_3\\ q_0 & -q_3 & q_2\\ q_3 & q_0 & -q_1\\ -q_2 & q_1 & q_0\end{bmatrix}\begin{bmatrix}p-b_p\\ q-b_q\\ r-b_r\end{bmatrix} \\ 0^{6\times1}\end{bmatrix}\end{aligned} \tag{16}$$

where, $X_s=[XYZuvwq_0q_1q_2q_3b_pb_qb_rb_{a_x}b_{a_y}b_{a_z}]^T$ is the state vector consisted of the 16 parameters; $u_m=[pqra_xa_ya_z]^T$, the system input measured by the rate gyroscope and accelerometer, is used to calculate state variables after error correction; ω is the white noise obeying normal distribution $N(0, Q)$; Q is the symmetric nonnegative variance matrix of ω; (X Y Z) is the UAV's location coordinates in the navigation coordinate system; (u v w) is the velocity of the UAV along the axis direction in the navigation coordinate system; ($q_0q_1q_2q_3$) is a quaternion used to describe the attitude of the UAV in the navigation coordinate system; ($b_pb_qb_r$) is the drift of three - axis rate gyroscope; ($b_{a_x}b_{a_y}b_{a_z}$) is the deviation of acceleration along the axis direction in the navigation coordinate system; g is the local gravity.

$$Z(t)=h(x_s)+v \tag{17}$$

where, $Z(t)$ is the system observation vector; $h(x_s)$ is the state observation function of the system observation vector; v is the white noise obeying normal distribution $N(0, Q)$; R is the symmetric positive definite variance matrix of ω. The system observation vector used to correct the location coordinates was shown in Eq. (18), and the state observation function in Eq. (19).

$$Z_1(t)=[X_{gps}Y_{gps}Z_{gps}U_{gps}V_{gps}W_{gps}]^T \tag{18}$$

$$h_1(x_s)=\begin{bmatrix}I_{3\times3} & 0_{3\times3}\\ 0_{3\times3} & T_{body}^{ned}\end{bmatrix}[X\ Y\ Z\ u\ v\ w]^T \tag{19}$$

where, ($X_{gps}Y_{gps}Z_{gps}$) is the value in the navigation frame transformed from GPS, which means transforming the value $\lambda\varphi h$ obtained in GPS from the WGS-84 frame into the navigation frame. ($U_{gps}V_{gps}W_{gps}$) is the velocity data in the navigation frame obtained from GPS.

Accelerometer and magnetometer are used as attitude reference to modify the attitude and flight path of UAV, which could be obtained by integrating the output of the three-axis rate gyroscope. The accelerometer and magnetometer could provide the reference of roll and pitch attitude and yaw by the gravitational acceleration component and geomagnetic component along the axial direction, respectively, in the body frame. Without considering the noise of measurement, the relationship between the parameters obtained from accelerometer and magnetometer and status parameter could be revealed in Eq. (20), Eq. (21) and Eq. (22). Where $\psi_{magnatometer}$ is the flight direction obtained by calculating the measurements of magnetometer. The calculation process is as follows. X^M, Y^M, Z^M, geomagnetic component along the axial direction in body frame, is substituted into Eq. (23) and Eq. (24) to obtain X_H, Y_H, geomagnetic component along the direction of X, Y axis in navigation frame. The flight direction could be obtained by Eq. (25). Where ϕ and θ are the roll and pitch angle obtained by calculating the measurements of accelerometer.

$$\phi=-\arctan 2(a_y,-a_z)=\arctan\left(\frac{2(q_0q_1+q_2q_3)}{q_0^2-q_1^2-q_2^2+q_3^2}\right) \tag{20}$$

$$\theta=\arctan 2\left(a_x,\sqrt{a_y^2+a_z^2}\right)=\arcsin(2(q_0q_2-q_1q_3)) \tag{21}$$

$$\psi=\psi_{magnatometer}=\arctan\left(\frac{2(q_0q_3+q_1q_2)}{q_0^2+q_1^2-q_2^2-q_3^2}\right) \tag{22}$$

$$X_H=X^M\cos\phi\,Y^M\sin\theta\sin\phi-Z^M\cos\theta\sin\phi \tag{23}$$

$$Y_H=Y^M\cos\theta+Z^M\sin\theta \tag{24}$$

$$\psi_{magnatometer}=\operatorname{atan}(Y_H/X_H) \tag{25}$$

The observation vector and the state observation function of the modified attitude are shown respectively in Eq. (26) and Eq. (27).

$$Z_2(t)=\begin{bmatrix} -\arctan 2(a_y,-a_z) \\ \arctan 2(a_x,\sqrt{a_y^2+a_z^2}) \\ \psi_{magnatometer} \end{bmatrix} \tag{26}$$

$$h_2(x_s)=\begin{bmatrix} \arctan\left(\dfrac{2(q_0q_1+q_2q_3)}{q_0^2-q_1^2-q_2^2+q_3^2}\right) \\ \arctan(2(q_0q_2-q_1q_3)) \\ \arctan\left(\dfrac{2(q_0q_3+q_1q_2)}{q_0^2+q_1^2-q_2^2+q_3^2}\right) \end{bmatrix} \tag{27}$$

Since Eq. (16), Eq. (19) and Eq. (27) are nonlinear continuous equations, it is necessary to linearize and discretize them before using the Kalman filter basic equations.

2.5 Linearization and discretization of the UAV's mathematical model

The first order derivative of Taylor series expansion is used to linearize the state function and observation function. The Taylor series of the system state function $f(x_s, u_m)$ is expanded at the point of $\hat{x}_{s(k-1)}$, the estimate of previous moment, and then the first-order partial derivative is obtained to form the Jacobian matrix F as shown in Eq. (28). Since this system is a continuous system, the series is expanded at x_0, the initial value of the system state, during the first Taylor series expansion. The obtained linear equation is discretized and substituted into the Kalman filter basic equation, to obtain the state estimates of the next sampling period. When the second Taylor series is expanded, the state estimates obtained from the previous sampling period are used to proceed. And thus the state estimates for each sampling period could be obtained by successive iteration. The Jacobian matrix is shown in Eq. (29).

$$F=\frac{\partial f(x_s,u_m)}{\partial x_s} \tag{28}$$

$$F=\begin{bmatrix} 0_{3\times3} & F_{xv3\times3} & F_{xq3\times4} & 0_{3\times3} & 0_{3\times3} \\ 0_{3\times3} & F_{vv3\times3} & F_{vq3\times4} & F_{vb3\times3} & F_{va3\times3} \\ 0_{4\times3} & 0_{4\times3} & F_{qq4\times4} & F_{qb4\times3} & 0_{4\times3} \\ 0_{3\times3} & 0_{3\times3} & 0_{3\times4} & 0_{3\times3} & 0_{3\times3} \\ 0_{3\times3} & 0_{3\times3} & 0_{3\times4} & 0_{3\times3} & 0_{3\times3} \end{bmatrix} \tag{29}$$

The state equation after linearization can be expressed as Eq. (30). The state transition matrix could be obtained by solving the first order nonhomogeneous linear differential equation and setting $\Delta t=t_k-t_{k-1}$, as is shown in Eq. (31). The transformation of system state variables from $F_{(k)}$ to matrix Φ_k realizes discretization. Where Δt is the sampling period.

$$\dot{X}(t)=FX(T)+W(t) \tag{30}$$

$$\Phi_{k,k-1}=e^{F\Delta t}\cong I+F\Delta t \tag{31}$$

Similarly, the partial derivative of the state observation function $g_i(x_s)$ with respect to x_s at the point of $\hat{x}_{s(k,k-1)}$ could form the corresponding Jacobian matrix, as is shown in Eq. (32) and Eq. (33).

$$H_1=\frac{\partial h_1(x_s)}{\partial x_s}=\begin{bmatrix} I_{3\times3} & 0_{3\times3} & 0_{3\times4} & 0_{3\times3}0_{3\times3} \\ 0_{3\times3} & H_{vv3\times3} & H_{vq3\times4} & 0_{3\times3}0_{3\times3} \end{bmatrix} \tag{32}$$

$$H_2=\frac{\partial h_2(x_s)}{\partial x_s}=[0_{3\times3}\ \ 0_{3\times3}\ \ H_{qq3\times4}\ \ 0_{3\times3}\ \ 0_{3\times3}] \tag{33}$$

The formulas used in Eq. (29) are as shown in the following equations.

$$F_{xv}=\begin{bmatrix} q_0^2+q_1^2-q_2^2-q_3^2 & 2(q_1q_2-q_0q_3) & 2(q_1q_3+q_0q_2) \\ 2(q_1q_2+q_0q_3) & q_0^2-q_1^2+q_2^2-q_3^2 & 2(q_2q_3-q_0q_1) \\ 2(q_1q_3-q_0q_2) & 2(q_2q_3+q_0q_1) & q_0^2-q_1^2-q_2^2+q_3^2 \end{bmatrix} \tag{34}$$

$$F_{vv}=\begin{bmatrix} 0 & b_r-r & q-b_q \\ r-b_r & 0 & b_p-p \\ b_q-q & p-b_p & 0 \end{bmatrix} \tag{35}$$

$$F_{vq}=2g\begin{bmatrix} -q_2 & q_3 & -q_0 & q_1 \\ q_1 & q_0 & q_3 & q_2 \\ q_0 & -q_1 & -q_2 & q_3 \end{bmatrix} \tag{36}$$

$$F_{qq}=\frac{1}{2}\begin{bmatrix} 0 & b_p-p & b_q-q & b_r-r \\ p-b_p & 0 & r-b_r & b_q-q \\ q-b_q & b_r-r & 0 & p-b_p \\ r-b_r & q-b_q & b_p-p & 0 \end{bmatrix} \tag{37}$$

$$F_{vb}=\begin{bmatrix} 0 & -w & w \\ w & 0 & -u \\ -v & u & 0 \end{bmatrix} \tag{38}$$

$$F_{qb}=\frac{1}{2}\begin{bmatrix} q_1 & q_2 & q_3 \\ -q_0 & q_3 & -q_2 \\ -q_3 & -q_0 & q_1 \\ q_2 & -q_1 & -q_0 \end{bmatrix} \tag{39}$$

$$F_{va}=\frac{1}{2}\begin{bmatrix} -1 & 0 & 0 \\ 0 & -1 & 0 \\ 0 & 0 & -1 \end{bmatrix} \tag{40}$$

$$F_{xq}=\begin{bmatrix} 2(q_0u-q_3v+q_2w) & 2(q_1u+q_2v+q_3w) & 2(-q_2u+q_1v+q_0w) & 2(-q_3u-q_0v+q_1w) \\ 2(q_3u+q_0v-q_1w) & 2(q_2u-q_1v-q_0w) & 2(q_1u+q_2v+q_3w) & 2(q_0u-q_3v+q_2w) \\ 2(-q_2u+q_1v+q_0w) & 2(q_3u+q_0v-q_1w) & 2(-q_0u+q_3v-q_2w) & 2(q_1u+q_2v+q_3w) \end{bmatrix} \tag{18}$$

$$H_{vv}=\begin{bmatrix} q_0^2+q_1^2-q_2^2-q_3^2 & 2(q_1q_2-q_0q_3) & 2(q_1q_3+q_0q_2) \\ 2(q_1q_2+q_0q_3) & q_0^2-q_1^2+q_2^2-q_3^2 & 2(q_2q_3-q_0q_1) \\ 2(q_1q_3-q_0q_2) & 2(q_2q_3+q_0q_1) & q_0^2-q_1^2-q_2^2+q_3^2 \end{bmatrix} \tag{19}$$

$$F_{vq}=\begin{bmatrix} 2(q_0u-q_3v+q_2w) & 2(q_1u+q_2v+q_3w) & 2(-q_2u+q_1v+q_0w) & 2(-q_3u-q_0v+q_1w) \\ 2(q_3u+q_0v-q_1w) & 2(q_2u-q_1v-q_0w) & 2(q_1u+q_2v+q_3w) & 2(q_0u-q_3v+q_2w) \\ 2(-q_2u+q_1v+q_0w) & 2(q_3u+q_0v-q_1w) & 2(-q_0u+q_3v-q_2w) & 2(q_1u+q_2v+q_3w) \end{bmatrix} \tag{20}$$

$$H_{qq}=\begin{bmatrix} \dfrac{2(q_1A_3-q_0A_2)}{A_3^2(1+A_1^2)} & \dfrac{2(q_0A_3+q_1A_2)}{A_3^2(1+A_1^2)} & \dfrac{2(q_3A_3+q_2A_2)}{A_3^2(1+A_1^2)} & \dfrac{2(q_2A_3-q_3A_2)}{A_3^2(1+A_1^2)} \\ \dfrac{2q_2}{\sqrt{1-B^2}} & \dfrac{-2q_3}{\sqrt{1-B^2}} & \dfrac{2q_0}{\sqrt{1-B^2}} & \dfrac{-2q_1}{\sqrt{1-B^2}} \\ \dfrac{2(q_3C_3-q_0C_2)}{C_3^2(1+C_1^2)} & \dfrac{2(q_2C_3-q_1C_2)}{C_3^2(1+C_1^2)} & \dfrac{2(q_1C_3+q_2C_2)}{C_3^2(1+C_1^2)} & \dfrac{2(q_0C_3+q_3C_2)}{C_3^2(1+C_1^2)} \end{bmatrix} \tag{44}$$

where, $A_2 = 2(q_0q_1 + q_2q_3)$, $A_3 = q_0^2 - q_1^2 - q_2^2 + q_3^2$, $A_1 = \frac{A_2}{A_3}$, $B = 2(q_0q_2 - q_1q_3)$, $C_2 = 2(q_0q_3 + q_1q_2)$, $C_3 = q_0^2 + q_1^2 - q_2^2 - q_3^2$, $C_1 = \frac{C_2}{C_3}$.

2.6 Estimation based on extended Kalman filter equation

The multi-sensors observation in the INS/GPS integrated navigation system required the data fusion using the algorithm to obtain the accurate state estimation. This paper selected the EKF algorithm as the data fusion algorithm, it was the derivative algorithm of Kalman filter to solve the filtering problem of stochastic nonlinear system. The essence of Kalman filter and its derivative algorithm is predicting the current state information based on the state estimation of previous time to obtain the predicted value of current state, and the predicted value was corrected by the current state observation to obtain the current accurate state estimation. In the integrated navigation system, the position information was predicted by accelerometer and corrected by the observation from GPS; the attitude information was predicted by gyroscope and the roll and pitch was corrected by the observation of accelerometer, the yaw was corrected by the magnetometer. The system state equation and observation equation were non-linear function, its linearization was achieved through the Taylor series expansion and the first order approximation.

After linearization and discretization of stochastic nonlinear continuous state equations and observation equations, one-step state transition matrix $\Phi_{k,k-1}$ and Observation matrix H_k could be formed. The flight state parameters could be estimated when $\Phi_{k,k-1}$ and H_k are substituted into Kalman filtering equation. State estimation can be divided into two processes: time update process and observation update process. The time update equation is shown in Eq. (45) and Eq. (46).

$$\hat{x}_{s(k,k-1)} = \hat{x}_{s(k-1)} + \int f(x_s(t), u_m(t))dt \quad (45)$$

$$P_{k,k-1} = \Phi_{k,k-1}P_{k-1}\Phi_{k,k-1}^T + Q_{k-1} \quad (46)$$

In the process of integral solving in Eq. (45), the fourth-order Longge-Kuta integral is used to improve the accuracy. The detailed solution process is shown in Eq. (47)-(51).

$$\Delta x_1 = f[x(t_{k-1})]T \quad (47)$$

$$\Delta x_2 = f[x(t_{k-1}) + \Delta x_1 / 2]T \quad (48)$$

$$\Delta x_3 = f[x(t_{k-1}) + \Delta x_2 / 2]T \quad (49)$$

$$\Delta x_4 = f[x(t_{k-1}) + \Delta x_3]T \quad (50)$$

$$\hat{x}_{s(k,k-1)} = \hat{x}_{s(k-1)} + (\Delta x_1 + 2\Delta x_2 + 2\Delta x_3 + \Delta x_4)/6 \quad (51)$$

The observation update equation is shown in Eq. (52)-(54).

$$K_k = P_{k,k-1}H_k^T[H_kP_{k,k-1}H_k^T + R_i]^{-1} \quad (52)$$

$$\hat{X}_{s(k)} = \hat{x}_{s(k,k-1)} + K_k[Z_{i(k)} - h_i(\hat{x}_{s(k,k-1)})] \quad (53)$$

$$P_k = [I - K_kH_k]P_{k,k-1} \quad (54)$$

3 Experiment and simulation analysis

3.1 Experimental general situation

On June 3, 2016, the test of UAV position and attitude detection was held in soybean test field in Jilin Agricultural University. The test field is located in Jingyue District of Changchun, Jilin province, China. The day of the test was cloudless. A suitable flight area is selected for the soybean test field, the path planning for the UAV is carried out, the GPS coordinates of the planned path are collected, the UAV is programmed to fly autonomously along the preset path, and the experimental data are collected by fixed-point aerial photography.

3.2 Experimental data analysis module

The experimental data analysis module includes three parts: flight path, flight altitude and attitude angle. "Flight path" outputs the actual and preset paths of the UAV, and shows whether and to what extent the actual flight location deviates from the preset one; similarly, "flight altitude" shows the altitude variation of the UAV during the flight. It could reflect the deviation between the actual flight height and the preset value, and thus the stability of the UAV altitude; "Attitude angle" shows the change of the rolling, pitching and yawing angle during the flight. It can be used to analyze whether the UAV can fly straight steadily, right-angle turn smoothly, and keep its attitude stabilized after turning.

3.3 Simulation Analysis

In this study, LabVIEW2013 language is used to simulate the experimental data, such as the change of attitude, position and flying height of UAV in the course of flying, hovering and fixed-point landing. Based on the original data obtained from flight test images, the control accuracy of the UAV was analyzed. The extended Kalman filter algorithm is used in offline optimization of the system state estimation. All sensor data was sent back to the ground station or on-board controller in real time and fused with the extended Kalman filter algorithm to estimate the location and attitude information more accurately, which provides real-time basis for controlling the flight status. The comparison of flight path map and attitude change map before and after the optimization will be used to analyze the effect of the extended Kalman filter algorithm in location and attitude control of UAV, which could provide a theoretical basis for applying the algorithm to actual flights of UAV. The main interface of LabVIEW, also of location and attitude measurement system, includes experimental data analysis module and EKF algorithm optimization module.

Input the experimental data obtained on June 3, 2016 into experimental data analysis module and the results are shown in Figures 4-8. According to the simulation results, actual flight path deviates from the preset one obviously, which reflects relatively low location control accuracy. The attitude control accuracy is good, the roll angle remains basically unchanged during the flight, and the pitch angle fluctuates within 10° deviation and remains stable during straight-line flight. The yaw angle shows UAV can achieve rapid and accurate steering. The flight attitude fluctuates within 1 meter throughout the flight, while within 0.5 meter during straight-line flight. The extreme point of flight attitude appears when steering.

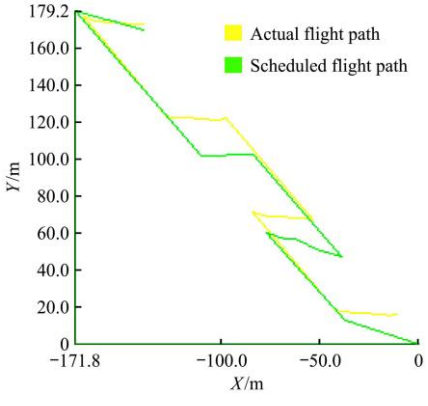

Figure 4 Flight path plo

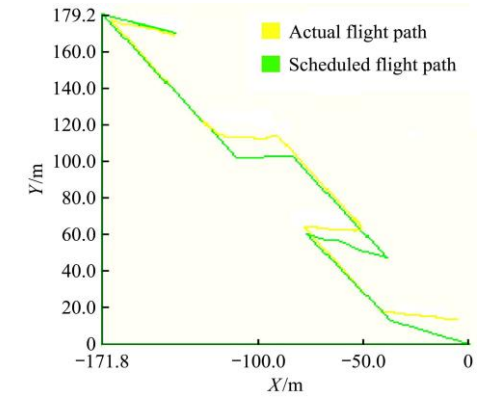

Figure 5 Flight path plot based on EKF algorithm

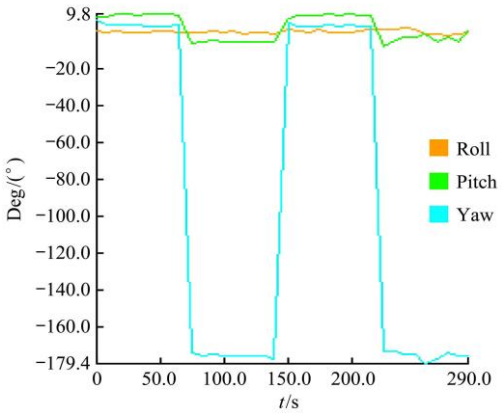

Figure 6 Attitude change plot

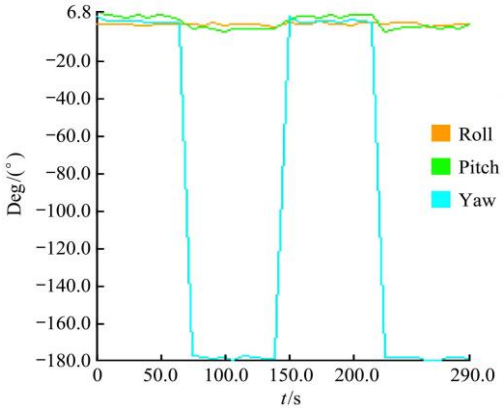

Figure 7 Attitude change plot based on EKF algorithm

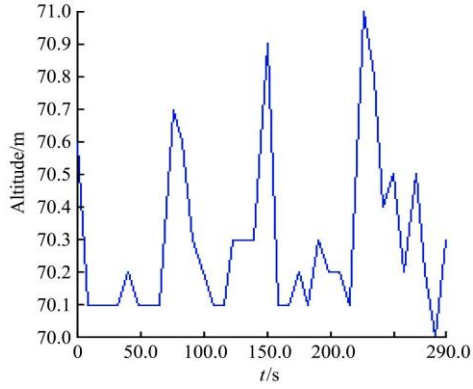

Figure 8 Flight attitude

The steering control accuracy of UAV is improved with the application of EKF algorithm. The flight path based on EKF is more consistent with the preset path, the pitch angle more stable and the yaw angle approaches closer to 180°.

4 Conclusions

Aiming for fast and accurate control of a UAV's position and attitude in precision agriculture, this study attempts to improve the estimation accuracy of position and attitude. The combination navigation system of INS/GPS (Inertial Navigation System/Global Positioning System) and EKF (Extended Kalman Filter) were adopted as a simulated navigation system and fusion algorithm respectively, to improve the estimation accuracy of UAV position and attitude.

Design of the detection system for a UAV's position and attitude in the LabVIEW environment to show UAV autonomous flight state and optimization effect of EKF algorithm with intuitive graphical forms. This system could also provide a theoretical basis for applying the EKF algorithm to real-time detection of UAV position and attitude by on-board controller.

Acknowledgments

This work were financially supported by National Natural Science Foundation of China (No.31501218) and National Key R&D Program of China (No.2016YFD0200701-1).

[References]

[1] Lan Y B, Chen S D, Bradley K Fritz. Current status and future trends of precision agricultural aviation technologies. Int J Agric Biol. 2017; 10(3).

[2] Ferry Bachmann, Ruprecht Herbst, Robin Gebbers, Verena V. Hafner. Micro UAV based georeferenced orthophoto generation in VIS+ NIR for precision agriculture. International Archives of the Photogrammetry, Remote Sensing and Spatial Information Sciences, 2013; XL-1:11–16.

[3] Sebastian Candiago, Fabio Remondino, Michaela De Giglio, Marco Dubbini, MarioGattelli. Evaluating Multispectral Images and Vegetation Indices for Precision Farming Applications from UAV Images. Remote Sens, 2015; 7(4): 4026–4047.

[4] Mohamar Moussa Ouédraogo, AuroreDegré, Charles Debouche, Jonathan Lisein. The evaluation of unmanned aerial system-based photogrammetry and terrestrial laser scanning to generate DEMs of agricultural watersheds. Geomorphology, 214 (2014): 339–355.

[5] Psiaki M L, Martel F, Pal P K. Three-axis Attitude Determination Via Kalman Filtering of Magnetometer Data. Journal of Guidance, Control, and Dynamics, 1990; 13(3): 506–514.

[6] Bar-Itzhack I Y, Oshman Y. Attitude Determination from Vector Observations: Quaternion Estimation. IEEE Transactions on Aerospace and Electronic Systems, 1985; AES-21(1): 128–136.

[7] Kumar N S, Jann T. Estimation of Attitudes from a Low-cost Miniaturized Inertial Platform using Kalman Filter-based Sensor Fusion Algorithm. Sadhana, 2004; 29(2): 217–235.

[8] Hall J K, Knoebel N B, McLain T W. Quaternion Attitude Estimation for Miniature Air Vehicles using a Multiplicative Extended Kalman Filter. Proceedings of the IEEE/ION Position, Location and Navigation Symposium 2008, Monterey, CA, 2008: 1230–1237.

[9] Cordova Alarcon J, Rodriguez Cortes H, Vivas E V. Extended Kalman Filter Tuning in Attitude Estimation from Inertial and Magnetic Field Measurements. Proceedings of the 6th International Conference on Electrical Engineering, Computing Science and Automatic Control, Toluca, Mexico, 2009: 1–6.

[10] Wang H Y, Djamaleddine Azaizia, CunyueLu, Baomin Zhang, Xun Zhao. Hardware in the Loop Based 6DoF Test Platform for Multi-rotor UAV. The 2017 4th International Conference on Systems and Informatics (ICSAI 2017): 1693–1697.

[11] W. Premerlani, P. Bizard. Direction cosine matrix IMU: Theory.DIY DRONE USA, 2009.

[12] HåvardFjær Grip, Thor I. Fossen, Tor A. Johansen, Ali Saberi. Globally exponentially stable attitude and gyro bias estimation with application to GNSS/INS integration. Automatica, 51(2015): 158–166.

[13] Ye. Somov, C. Hacizade, S. Butyrin. In-orbit Calibration of Attitude Determination Systems for Land-survey Micro-satellites. The International Federation of Automatic Control Cape Town, 2014; 7941–7946.

[14] Sreejith A G., Joice Mathew, Mayuresh Sarpotdar, Rekhesh Mohan, AkshataNayak, Margarita Safonova, etc. A Raspberry Pi-Based Attitude Sensor. Journal of Astronomical Instrumentation, 2014; 3(2): 1440006.

[15] Zheng Sheng. Virtual Instrumentation Technology and its Evolution. Foreign Electronic Measurement Technology, 1997(2): 40–44.